US/GR BK/

SUMMER STUDENT LECTURE 1972

"The Pulsating Radio Stars"

D. C. Backer

DISCOVERY

In 1967 a group of scientists in Cambridge, England undertook a systematic study of the effects of the interplanetary medium on the propagation of radiation from compact extragalactic sources. For this purpose they constructed a multi-acre array of dipole antennae and began recording the interplanetary scintillations of all sources in the sky. The novel aspect of these observations was that they demanded very little smoothing of the data to detect the rapid scintillations. For this reason they were the first to survey the sky for sources which were varying rapidly for reasons other than scintillation. A student on the project noted a source of pulsed radiation that recurred day after day. The pulsations were accurately periodic and had a duty cycle of about 3%. For three months this object was followed with the utmost of secrecy. After that time they were certain of its cosmic origin for two reasons: it maintained the same position in the sky which meant that it could not be a terrestrial event at the same time each day, and the observed period of the pulsations changed in a way consistent with the variations expected from the Doppler shift of the observatory due to the orbital motion of the Earth about the Sun. Thus their systematic study led to the discovery of a new and unexpected source of radio radiation.

Later investigations by the Cambridge group and by scientists at the Mills' Cross in Australia, at Jodrell Bank in England, at the NRAO and at the Arecibo Observatory have resulted in a list of 65 pulsating radio sources or pulsars. A current list is given in Table I. The accurate periodicity of the signals from the pulsars is their most distinctive property. The periods are frequently determined to one part in 10^9. This is the accuracy that quartz crystals can be made to oscillate in the laboratory. In astrophysics, this accuracy implies that the phenomenon is in the realm of the mechanics of massive bodies since only these bodies have the inertia to maintain some form of motion with precision. Standard questions about massive objects for the astrophysicist are: what is the characteristic time scale of a body in relation to its mass and radius; and what are the possible equilibrium states, which are required so that we can expect to view them, of stellar masses. With regard to the latter question, it has been known for many years that the dying embers of a star could form a <u>white dwarf</u> with its mass supported against the gravitational collapse which is expected in a star which has exhausted its nuclear fuel by an electron degeneracy pressure. These objects had been detected amongst the local stars. Around 1940, as a byproduct of atomic bomb research, it was predicted that a <u>neutron star</u> might exist; its mass would be supported against collapse by a nuclear degeneracy pressure. Later it was suggested that these objects might be formed in supernova explosions. Recently much interest has been devoted to an additional object where the collapse could not be averted; the mass disappears into a <u>black hole</u>, so called since light cannot escape from the surface of the object. An envelope calculation of the vibrational time scale for these objects is found by setting the gravitational acceleration at the surface GM/R^2 equal to an acceleration of the surface written as R/t^2. This results in $t \sim (G\rho)^{-1/2}$ where ρ is the density M/R^3. A similar calculation for rotation comes from setting the surface gravitational acceleration equal to the centrifugal force. This results in the same estimate for t. For the tremendous density of 10^{14} gm/cm^2, which has been suggested for neutron stars, t ~ 1 ms.

Another speculation about these star embers is that the magnetic fields would be large as a result of the collapse or implosion of a large star down to a white dwarf or neutron star. Consider the Sun with a one Gauss field ($B_\odot$). Now allow the Sun to contract from R_o to a radius R while conserving flux: $\Phi \sim B_\odot R_\odot^{\,2} \sim B R^2$. The new field $B \sim B_\odot R_\odot^{\,2}/R^2$. This results in predictions of 10^6 Gauss for white dwarfs ($R \sim 10^8$ cm), which has been measured in one white dwarf, and 10^{11} Gauss for neutron stars ($R \sim 10^6$ cm).

Considering the matrix of attractive possibilities, white dwarf/neutron star and rotation/vibration, Professor Gold was convinced that the objects were rotating, magnetic neutron stars. In his model the magnetic field is forced into corotation by magnetohydrodynamic forces arising from its plasma content. However this "magnetosphere" of the neutron star would run into trouble at a distance from the axis of rotation R_c where the corotation at constant angular frequency Ω forces the field and plasma to the speed of light, $R_c = c/\Omega$. Gold felt that there would be some interaction on this "light cylinder" causing the corotation to stop and producing anisotropic radio radiation which we view as pulses just as one views a revolving beacon from a lighthouse. The great prediction of this model was that the pulsar periods would decay with time due to a loss of rotational energy. This was contrasted with vibrational models where energy loss leads to collapse, to higher densities, and hence to shorter period oscillations. Furthermore, Gold predicted that, since the time scale t for neutron stars could extend down to 1 ms, young, short period pulsars remained to be detected. Both the period increase with time and a young short period pulsar were detected.

PROPAGATION PHENOMENA

The pulsar emission arrives in short pulses when observed with a narrow bandwidth at any radio frequency. A comparison of the outputs from two such bandwidths with center frequencies offset by a few MHz shows that the pulses arrive at a later time at lower frequencies. When extension is made to larger frequency offsets, it is found that the delay between pulses has a quadratic dependence on frequency. Because the pulse arrival time is frequency dependent we say the pulsar radiation is dispersed. The microscopic interaction between electromagnetic waves and matter in the transmitting medium causes a wave packet to travel at speeds less than c; that is, the group velocity is less than c. If the interaction is frequency dependent, the medium is called dispersive. A plasma is a dispersive medium and from Maxwell's equations one can find a dispersion relation between the index of refraction and the radio frequency. From this the group velocity is derived. For a plasma with only the interaction with the electrons considered and with negligible magnetic field this relation is

$$v_g/c = 1 - n_e\, e^2/(2\pi\, m_e\, c^2\, \nu^2)$$

The dispersion delay between frequencies ν_1 and ν_2 is

$$\tau_d = (1/\nu_2^{\,2} - 1/\nu_1^{\,2})\, \frac{e^2}{2\pi m_e c} \int n_e\, d\ell$$

This relation accurately describes all observations of pulse arrival delay with frequency. The dynamic spectrum of a pulsar is sketched in Figure 1. The parameter $\int N_e \, d\ell$ has been defined as the <u>dispersion measure</u> (DM) with units of parsecs cm^{-3}. The observed range is

$$3 < \text{DM observed} < 400 \text{ pc cm}^{-3}$$

Where is this plasma? The following table will allow some statements to be made on various hypotheses.

MEDIUM	ELECTRON DENSITY	DEPTH	D.M. CONTRIBUTION	HYPOTHESIS TEST
Earth Ionosphere	$3x10^5$ cm^{-3}	$1.5x10^8$ cm	$5x10^{13}$	No
Interplanetary Medium (away from Sun)	1-10	AU=$1.5x10^{13}$	10^{14}	Yes
Instellar Medium	$\lesssim$0.1	300pc = 10^{21}	10^{20}	Yes
HII Regions	~1	~10 pc	$3x10^{19}$	Possible
Pulsar Neighborhood	Crab:40 Others?	0.5 pc	$6x10^{19}$	Yes No?

Further confidence in attributing the dispersion to the interstellar medium in the general case can be gained from the presentation in Figure 2, a correlation diagram of the DM and the galactic latitude b^{II}. The correlation is that expected if the pulsars reside in the plane of the galaxy and if the DM comes from plasma distributed in the plane. From the above discussion it is clear that, after corrections are made for obvious HII regions or pulsar associated nebulae, a reasonable distance estimate can be obtained by dividing the DM by the average electron density

$<n_e>$. It is certain the medium is not uniform, but on a statistical basis these estimates should be valid.

The nonuniformity of the medium plays an important role in the observations of pulsars. There is a simple appraoch to this which will serve to illustrate the relation between various parameters. The rays from a pulsar are bent by the plasma irregularities which act as giant lenses. This is a result of the microscopic scattering process described above. The rays observed are spread over an angle θ_s. Due to geometrical path length differences for rays arriving from angles extending to Θ_s, a pulse will be spread over a time τ_b. The mixture of signals with different delays gives rise to interference of the signal across the radio spectrum with a scale of $B_s \sim 1/\tau_b$ and a depth of modulation m. Finally if there is a velocity of the entire scattering medium relative to the pulsar-observer line of sight, from Earth, pulsar or medium motion, then the interference which also varies spatially at a fixed frequency will give rise to slow temporal variations with a time scale $\tau_s = a_p/v$; a_p is the interference pattern scale size and v is the relative velocity. Given this model of the phenomenon, two telescopes spaced by a large fraction of a_p will measure an offset in time of arrival of the same temporal variations $\Delta t = d/v$, where d is the projected separation of the telescopes.

Figure 3 is a sketch of the dynamic spectrum, with the axes compressed over that of Figure 1, which includes paths of individual dispersed pulses and constructive interference "islands" in the frequency-time plane. In Figure 4 the variations of the scale sizes of the islands, B_s and τ_s, and of the depth of modulation, m, with radio frequency are shown. Below ~1 GHz the medium severely modulates the radiation. The modulation measure m is unity, the bandwidth B_s varies as ν^4 and the time scale τ_s varies as ν. Above ~1 GHz m decreases as ν^{-1}, B_s increases less rapidly and τ_s is roughly constant. Figure 5 displays observational results for B_s and τ_b as a function of ν and DM. The quadratic dependence of B_s and τ_b^{-1} on DM is further proof that the dispersion comes from the general interstellar medium.

All of these phenomena are areas of current experimental and theoretical investigations. The simple theory indicates that the scale of the fluctuations is very small, ~10^{11} cm, which is difficult to reconcile with the knowledge of lifetimes of density irregularities of that scale.

INTRINSIC PHENOMENA

Many studies have been made of phenomena intrinsic to the radiation mechanism of the pulsar. A fundamental property of a radio source is the spectrum of its emission. For the pulsar an equivalent continuous flux density spectrum can be defined. These spectra have not been studied well; some estimates are given in Figure 6. The general features are a straight section in the region between 100 and 1000 MHz with slopes around -1 and turnovers toward the lower frequencies and toward the higher frequencies. Before discussing a cause for these features of the spectrum a few comments are needed about the general nature of the emission mechanism. A standard argument in astrophysics is that if the power from an object varies over a time t, then the size of the emitting region must be less than the light distance ct so that the emitting particles can communicate about variations. In the pulsars t is, for example; 100 μsec. For a 1000 flux unit emission level at a wavelength of one meter from a source at 300 pc, this implies a brightness temperature from the Planck law of 10^{28} °K. Such a temperature cannot be simple incoherent radiation since it would require charges whose energy is 10^{24} eV. Such energetic charges, if they could be produced, would radiate extremely high frequency photons, not radio waves. To explain the 10^{28} °K it is necessary to invoke a coherent radiation mechanism, one in which N charges move in unison and act as a single ion with charge N_e. This allows an enhancement of brightness temperature over incoherent mechanisms by a factor of $\sqrt{N}$. It is worth noting here that the one coherent source outside our solar system which was suggested before pulsars were discovered turned out to be a pulsar, the Crab Nebula pulsar. In fact it had been suggested in 1967 by Pacini that there was a spinning, magnetized neutron star in the Crab Nebula; unfortunately he did not consider that it might be equipped with a "bell".

The low frequency turnovers could be due to thermal absorption by the interstellar hydrogen, but they occur at frequencies somewhat higher than what standard galactic models would predict. A more likely mechanism is some form of self-absorption by the radiating charges causing a decrease of the emissivity with decreasing frequency. It is also possible that there is merely a lower limit to the spectrum of coherent emission.

The high frequency turnover is certainly related to the emission mechanism. The wavelength at which this occurs may relate to a minimum scale length for the coherent motion of the radiating charges. Certainly other models could be proposed.

An average of the radiation synchronously with the pulse period produces a pulse profile which is characteristic for each object. These often show the presence of components, or distinct regions within the pulse emission window. The different morphologies are displayed in Figure 7. These profiles are largely constant in time over intervals of a year. They can have weak dependences on radio frequency: the component separation and width often decrease slowly with increasing frequency. In several of the shortest period pulsars emission is detected nearly midway between pulses (Figure 8). These are called interpulses. Also in two objects, 0531+21 and 0950+08, there is emission throughout an interval between the main-pulse and interpulse known as the baseline component.

Our knowledge of the guts of a pulsar is in a primitive state. These components of the pulse may represent separate streams of charges from the central star which radiate in our direction once per pulse period as a consequence of the rotation. Another view is that the components represent a variation of the efficiency of the production of coherent radiation with angle across a wide stream of charges.

The extremely strong magnetic fields predicted are required in most models of the emission mechanisms to provide a means of accelerating the charges. The coherent motion of a large number of charges along a curved magnetic field line will produce high degrees of linear polarization in a direction parallel to the radius of curvature of the field. Large degrees of linear polarization are seen in pulsar radiation, in some cases as much as 100%. The angle of the polarization often varies slowly across the pulse. This variation has been shown to be similar over a wide range of frequencies which confirms the idea that the high degree of polarization is the result of charge acceleration in a non-uniform magnetic field. The polarization phenomena then is important for revealing the field structure in the emitting region.

The pulsar emission varies on every time scale that has been investigated. The minute-to-hour variations arising from propagation effects have already been discussed. The variations intrinsic to the pulsar emission range from micropulses which last for 10-100 μsec, or $0^\circ.015 - 0^\circ.03$ when measured in longitude, to subpulses which have a scale around 1° of longitude, to pulse to pulse variations. Beyond the variations lasting for a few pulse periods, there is a domain between 50 and a few hundred pulse periods. Finally recent studies have shown that the average flux of some pulsars varies on a weekly to monthly time scale and that the pulse profile can evolve slowly with time over a period of several months.

Much of the phenomenology of pulsar data has not been discussed. The many details of the Crab Nebula pulsar, its optical and X-ray radiation and its relation to the Nebula, ha~~s~~ve been omitted. No mention was made of investigations of local magnetic field strengths from Faraday rotation. Theoretical models were treated only lightly; in particular no comment was given about the solid state physics of neutron stars and its relation to observational quantities.

References to several review articles are given.

REFERENCES

A. Review

M. Ruderman 1971, Scientific American, **224**, No. 2.

J. Ostriker 1971, Scientific American, **224**, No. 1.

A. Hewish 1970, Ann. Rev. Ay. Ap., 8, p. 265.

Tilson 1970, IEEE Spectrum, Feb. 1970, p. 40.

IAU Symposium No. 46 Proceedings, 1970, Jodrell Bank.

B. Discovery

Pulsating Stars, two volumes of reprints from Nature.

C. Propagation Effects

Dispersion and Rotation Measures: R. N. Manchester 1972, Ap. J., **172**, 43.

Scintillation: B. J. Rickett 1970, M.N.R.A.S., **150**, 67.

K. R. Lang 1971, Ap. J., **164**, 249.

D. Intrinsic Phenomena

Spectra: Hewish above; D. C. Backer 1972, Ap. J. (Letters), **174**, L157.

Polarization: R. N. Manchester 1971, Ap. J. Suppl. Ser., **23**, 283.

Subpulse phenomena: J. H. Taylor, G. R. Huguenin 1971, Ap. J., **167**, 273.

A. G. Lyne, F. G. Smith, D. A. Graham 1971, M.N.R.A.S., **153**, 337.

ERVANT TERZIAN CRSR AND NAIC CORNELL UNIVERSITY *PULSARS* JUNE 20,1972 TOTAL NUMBER= 65 PAGE 1

ULSAR ESIGNATION	PILSAR	R.A. H.M.S.	DECL. DEG. ' "	L II DEG.	B II DEG.	PERIOD (SEC)	EPOCH (J.D.24+)	1/2 PULSE WIDTH (MSEC)	DISPERSION MEASURE (PARSEC/CM3)	PERIOD CHANGE (NSEC/DAY)	APP. AGE P/(DP/DT) (YRS)
0031-07	MP0031	0 31 36	-07 38 26	110.4	-69.8	0.9429507566	40690	51.0	10.89	0.0366	7.1E+07
0254-54	MP0254	2 54 24	-54	270.9	-54.9	0.4476	(41347)	10	10		
0301+19	PSR0301+19	3 01 45	19 22 00	161.1	-33.3	1.3875852	41347	42	15.5		
0329+54	CP0329	3 29 11	54 24 38	145.0	-1.2	0.71451864244	40622	6	26.776	0.177	1.1E+07
0450-18	MP0450	4 50 22	-18 04 14	217.1	-34.1	0.54893507	40938	26	25		
0525+21	NP0525	5 25 45	21 56 32	183.8	-6.9	3.745490813	40236	181.0	50.8	3.452	3.0E+06
0531+21	NP0531	5 31 31	21 58 55	184.6	-5.8	0.0331296454	41221	3	56.805	36.526	2.5E+03
0628-28	PSR0628-28	6 28 51	-28 34 08	237.0	-16.8	1.24441495981	40242	(50)	34.36	0.217	1.6E+07
0736-40	MP0736	7 36 51	-40 35 18	254.2	-9.2	0.374918324	40221	22	100	<1.728	>5.9E+05
0740-28	PSR0740-28	7 40 48	-28 15 16	243.8	-2.4	0.166750167	41027	8	80		
0809+74	CP0809	8 09 03	74 38 10	140.0	31.6	1.2922412852	40689	41.3	5.84	0.0138	2.5E+08
0818-13	MP0818	8 18 06	-13 40 57	235.9	12.6	1.2381245	(40618)	22	40.9		
0823+26	AP0823+26	8 23 51	26 47 18	197.0	31.7	0.530659599042	40242	5.9	19.4	0.144	1.0E+07
0833-45	PSR0833-45	8 33 39	-45 00 19	263.6	-2.8	0.0892187479	40307	2	63	10.823	2.3E+04
0834+06	CP0834	8 34 26	06 20 47	219.7	26.3	1.27376349759	40626	23.7	12.90	0.587	5.9E+06
0835-41	MP0835	8 35 34	-41 24 54	260.9	-0.3	0.76698	(41347)	20	120		
0904+77	PSR0904+77	9 04	77 40	135.3	33.7	1.57905	(40222)	<80			
0940-56	MP0940	9 40 40	-56	278.8	-2.5	0.662	(40402)	30	145		
0943+10	PP0943	9 43 20	10 05 33	225.4	43.2	1.097707	40519	50	15.35		
0950+08	CP0950	9 50 31	08 09 43	228.9	43.7	0.25306504317	40622	8.8	2.965	0.0198	3.5E+07
0959-54	MP0959	9 59 51	-54 37	280.1	0.3	1.436551	40553	50	90		
1055-51	MP1055-51	10 55 49	-51 40	286.0	7.0	0.1971	(41347)		<30		
1112+50	PSR1112+50	11 12 49	50 40	155.1	60.7	1.6564392	(41347)	15			
1133+16	CP1133	11 33 28	16 07 33	241.9	69.2	1.18791116405	40622	27.7	4.834	0.323	1.0E+07
1154-62	MP1154	11 54 45	-62 08 36	296.7	-0.2	0.40052	(41347)		270		
1237+25	AP1237+25	12 37 12	25 10 17	252.2	86.5	1.38244857195	40626	49.9	9.254	0.0825	4.6E+07
1240-64	MP1240	12 40 20	-64 07 12	302.1	-1.6	0.38850	(41347)	60	220		
1359-50	MP1359	13 59 43	-50	314.5	11.0	0.690	(40585)	20	20		
1426-66	MP1426	14 26 34	-66 09 54	312.3	-6.3	0.7874	(41347)	10	60		
1449-65	MP1449	14 49 22	-65	315.3	-5.3	0.180	(40282)	(5)	90		
1451-68	PSR1451-68	14 51 29	-68 32	313.9	-8.6	0.263376764	(40545)	25	8.6	<0.259	>2.8E+06
1508+55	HP1508	15 08 04	55 42 56	91.3	52.3	0.73967787630	40626	10.3	19.60	0.433	4.7E+06
1530-53	MP1530	15 30 23	-53 30	325.7	1.9	1.368852	40553	25	20		
1541+09	AP1541+09	15 41 14	09 38 43	17.8	45.8	0.7484483	(41347)	63	35.0		
1556-44	MP1556	15 56 12	-44 31 30	334.5	6.4	0.25705	(41347)				
1604-00	MP1604	16 04 37	-00 25 08	10.7	35.5	0.4218164	(40618)	15	10.72		
1642-03	PSR1642-03	16 42 25	-03 12 30	14.1	26.1	0.38763877965	40622	3.7	35.71	0.154	6.9E+06
1700-18	MP1700-18	17 00 56	-18	4.0	14.0	0.802	(41347)		<40		
1706-16	MP1706	17 06 33	-16 37 21	5.8	13.7	0.65305045437	40622	12	24.99	0.550	3.3E+06
1727-47	MP1727	17 27 50	-47 42 18	342.6	-7.6	0.829683	40553	30	121		
1747-46	MP1747	17 47 56	-46 56 12	345.0	-10.2	0.742349	40553	20	40		
1749-28	PSR1749-28	17 49 49	-28 06 01	1.5	-1.0	0.562553168299	40127	6	50.88	0.705	2.2E+06
1818-04	MP1818	18 18 14	-04 29 03	25.5	4.7	0.59807262183	40622	10.3	84.48	0.545	3.0E+06
1845-01	DP1845-01	18 45	-01 27	31.3	0.2	0.659475	(41192)	(80)	90		
1845-04	JP1845	18 45 10	-04 05 32	28.9	-1.0	0.59773452	40998	20	141.9		
1857-26	MP1857	18 57 44	-26 04 49	10.5	-13.5	0.612204	41026	25	35		
1858+03	JP1858	18 58 40	03 27 02	37.2	-0.6	0.655444	40754	(170)	402		
1911-04	MP1911	19 11 15	-04 45 59	31.3	-7.1	0.82593366503	(40624)	8.0	89.41	0.351	6.5E+06
1915+13	DP1915+13	19 15 00	13 50 00	48.2	0.7	0.1946255	41274	15	97		
1919+21	CP1919	19 19 36	21 47 17	55.8	3.5	1.33730115212	40690	31.2	12.43	0.116	3.2E+07
1929+10	PSR1929+10	19 29 52	10 53 03	47.4	-3.9	0.22651703833	40625	5.3	3.176	0.100	6.2E+06
1933+16	JP1933+16	19 33 32	16 09 58	52.4	-2.1	0.35873542051	40690	8.0	158.53	0.519	1.9E+06
1944+17	MP1944	19 44 39	17 58 44	55.3	-3.5	0.4406179	(40618)	30	35		
1946+35	JP1946	19 46 35	35 30	70.6	5.1	0.717306	40659	21	129.1		
1953+29	JP1953	19 53 00	29 15 03	66.0	0.7	0.426676	40754	13	20		
2003+31	JP2003	20 03 00	31 30	69.0	0.0	2.111206	40756	25	225		
2016+28	AP2016+28	20 16 00	28 30 31	68.1	-4.0	0.55795339053	40689	13.9	14.16	0.0129	1.2E+08
2020+28	PSR2020+28	20 20 33	28 44 39	68.9	-4.7	0.34340072	40968	15			
2021+51	JP2021	20 21 25	51 45 09	87.9	8.4	0.52919531221	40626	6.6	22.580	0.263	5.5E+06
2045-16	PSR2045-16	20 45 47	-16 27 48	30.5	-33.1	1.96156682076	40695	79.0	11.51	0.945	5.7E+06
2111+46	JP2111	21 11 41	46 36	89.1	-1.2	1.0147777	(40509)	29	141.4		
2154+40	PSR2154+40	21 54 56	40 00	90.5	-11.5	1.525264	(41347)	50	110		
2217+47	PSR2217+47	22 17 46	47 39 48	98.4	-7.6	0.53846737844	40624	7.9	43.52	0.239	6.2E+06
2303+30	AP2303+30	23 03 30	30 45	97.7	-26.6	1.575869	(40402)	26.0	49.9		
2319+60	JP2319	23 19 42	60 00	112.0	-0.6	2.256483	40734	140	96		

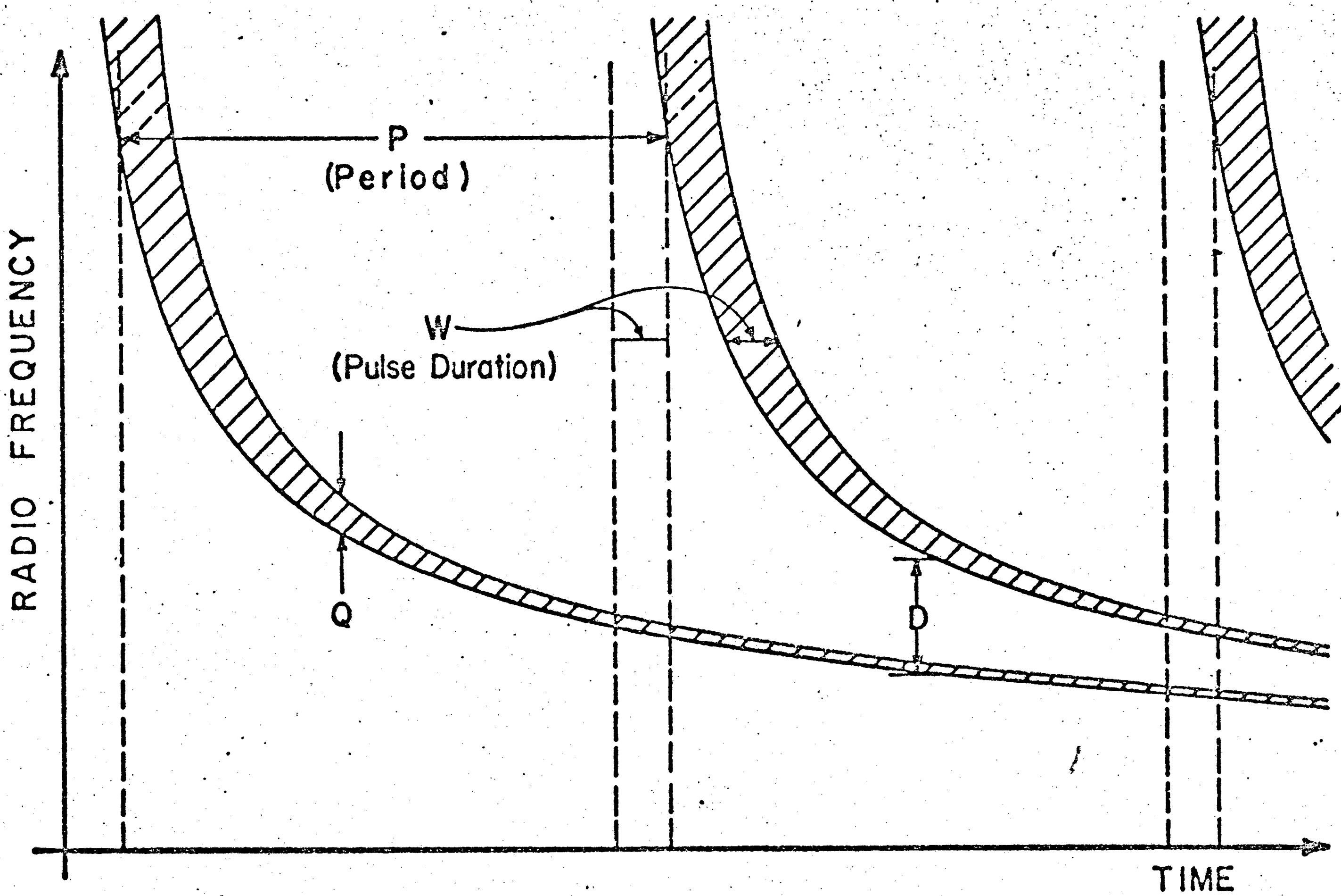

Pulsar Dynamic Spectrum. The hatched area indicates region of the frequency-time plane that is occupied by a series of pulses.

Figure 1

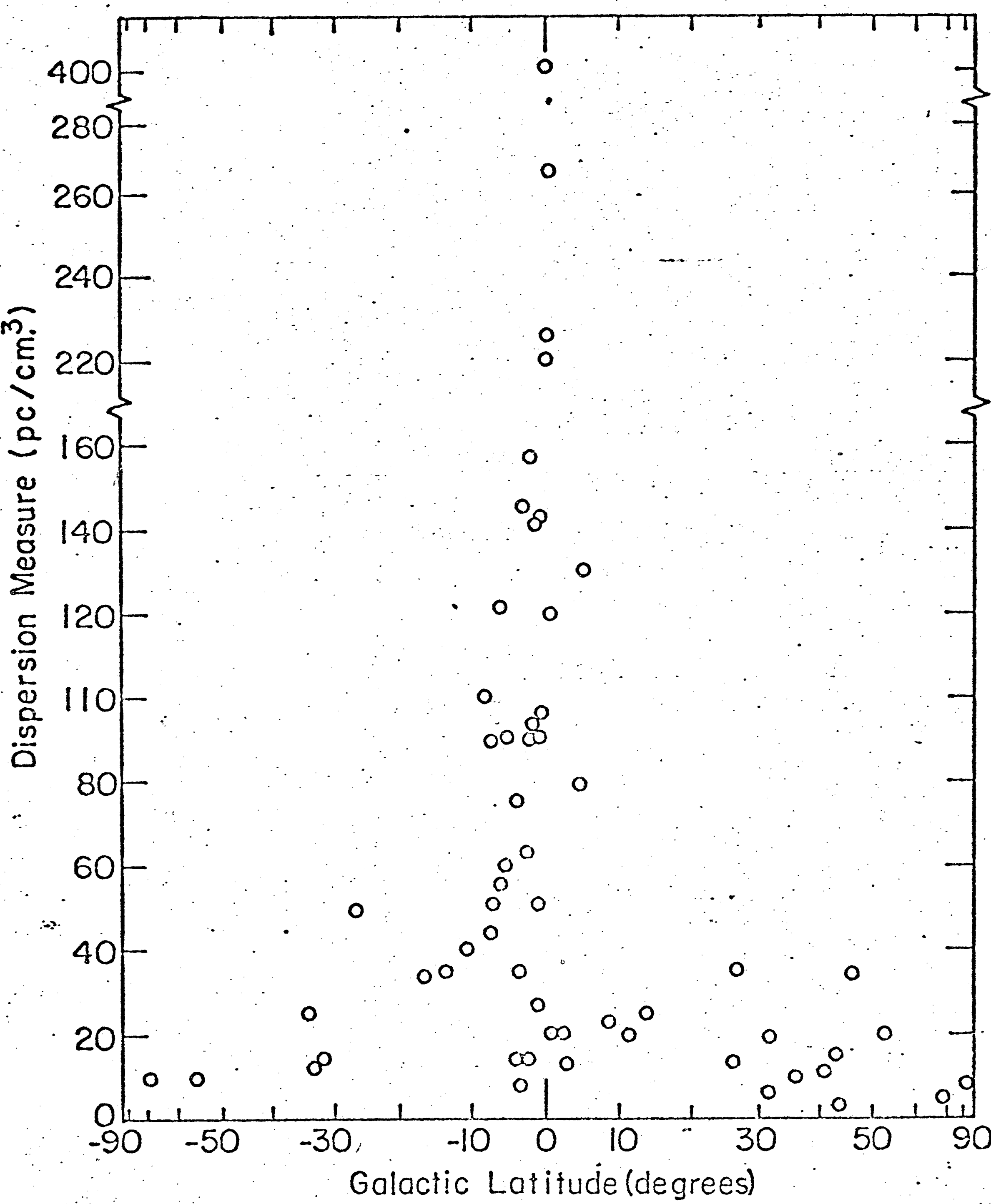

Correlation Diagram - Dispersion Measure and Galactic Latitude.

Figure 2

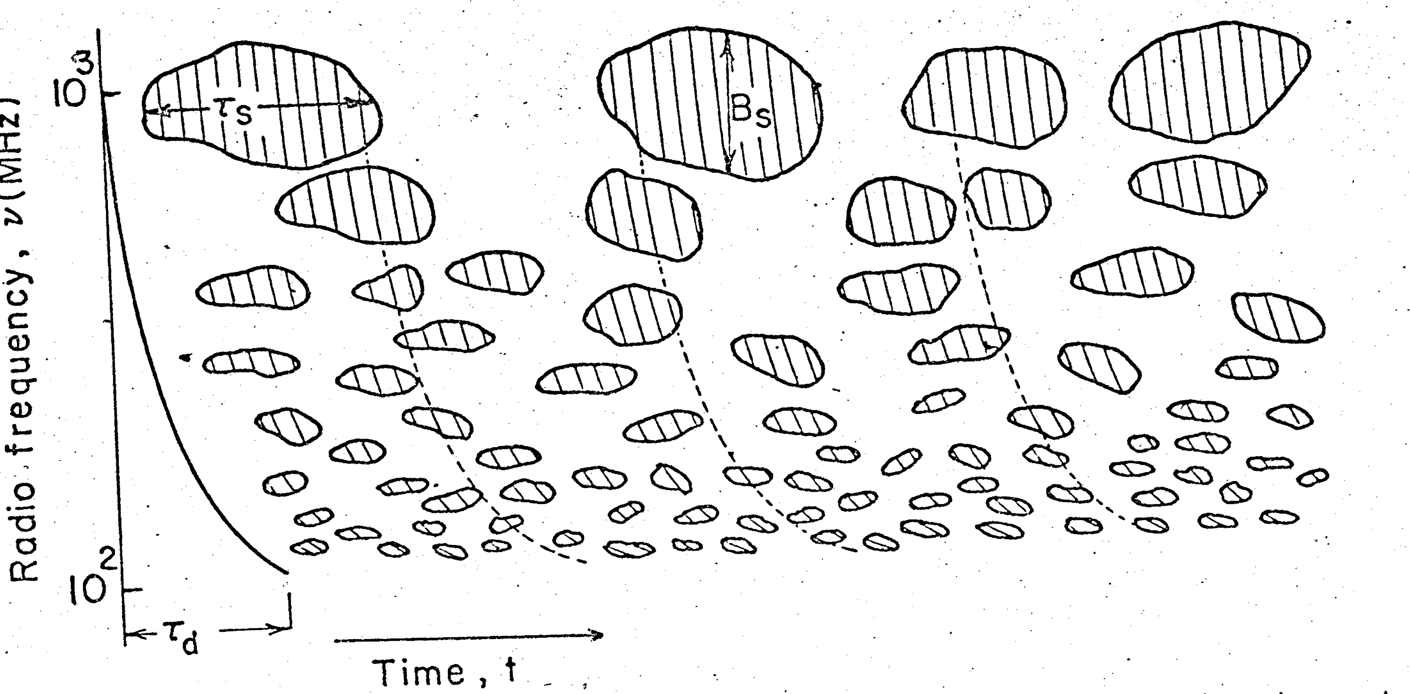

Pulsar Dynamic Spectrum. The pulsar signal is only observed within "interference islands" caused by propagation in the interstellar medium.

Figure 3

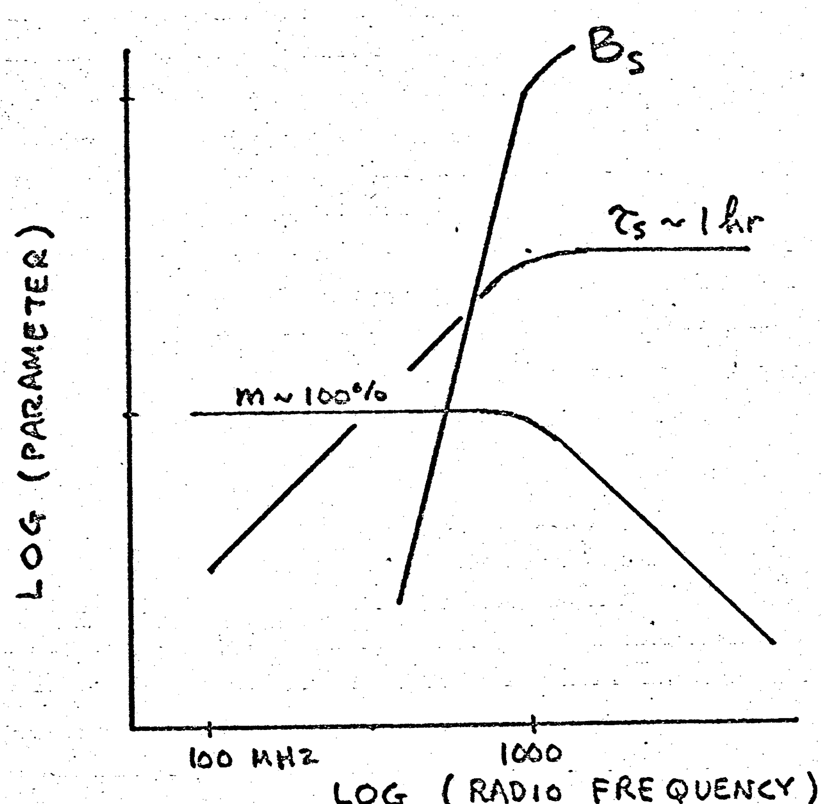

Variation of the scale of the "interference islands" B_s and τ_s and the depth of modulation m with frequency - typical pulsar.

Figure 4

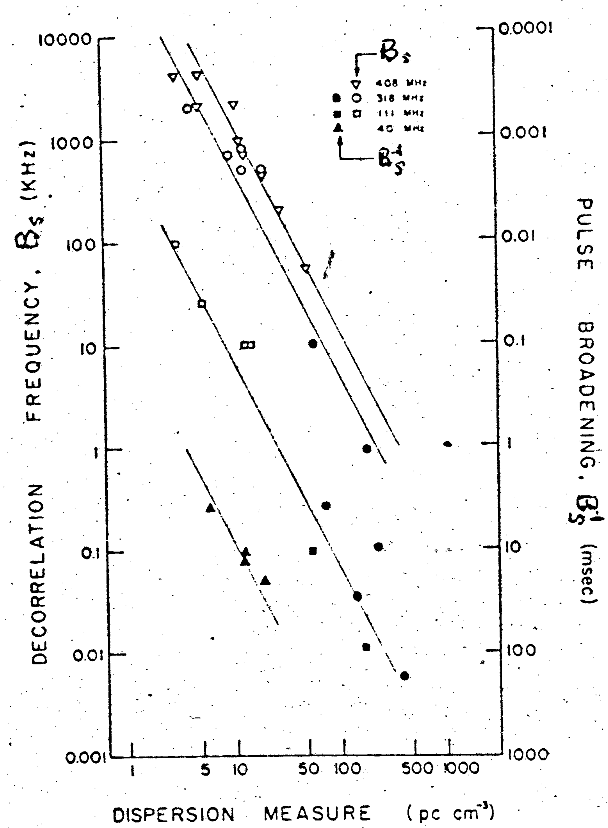

Observed Scintillation Parameters as a function of ν and DM.

Figure 5

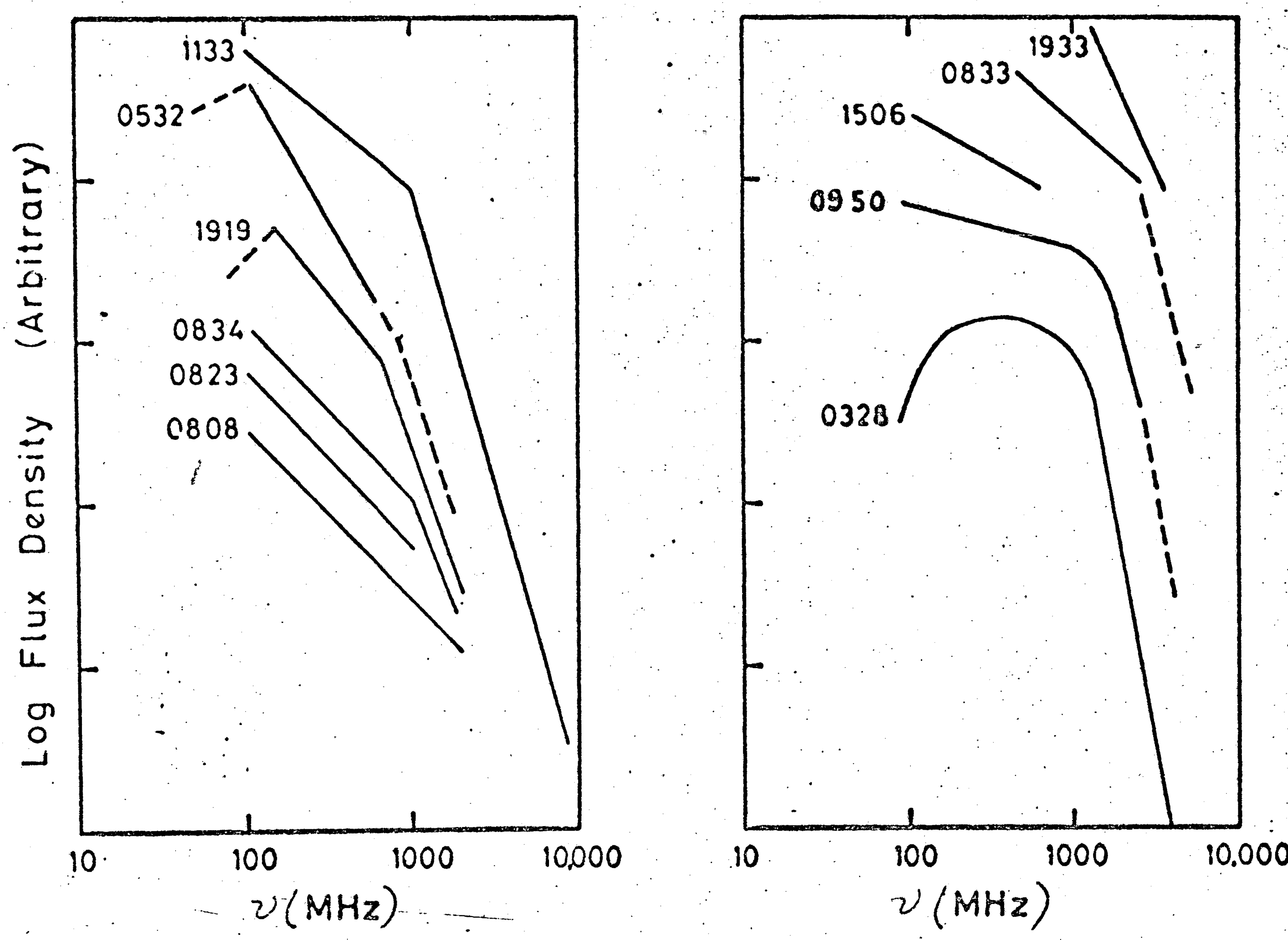

Flux Density Spectra. Estimates of the equivalent continuum flux density spectrum for 11 pulsars.

Figure 6

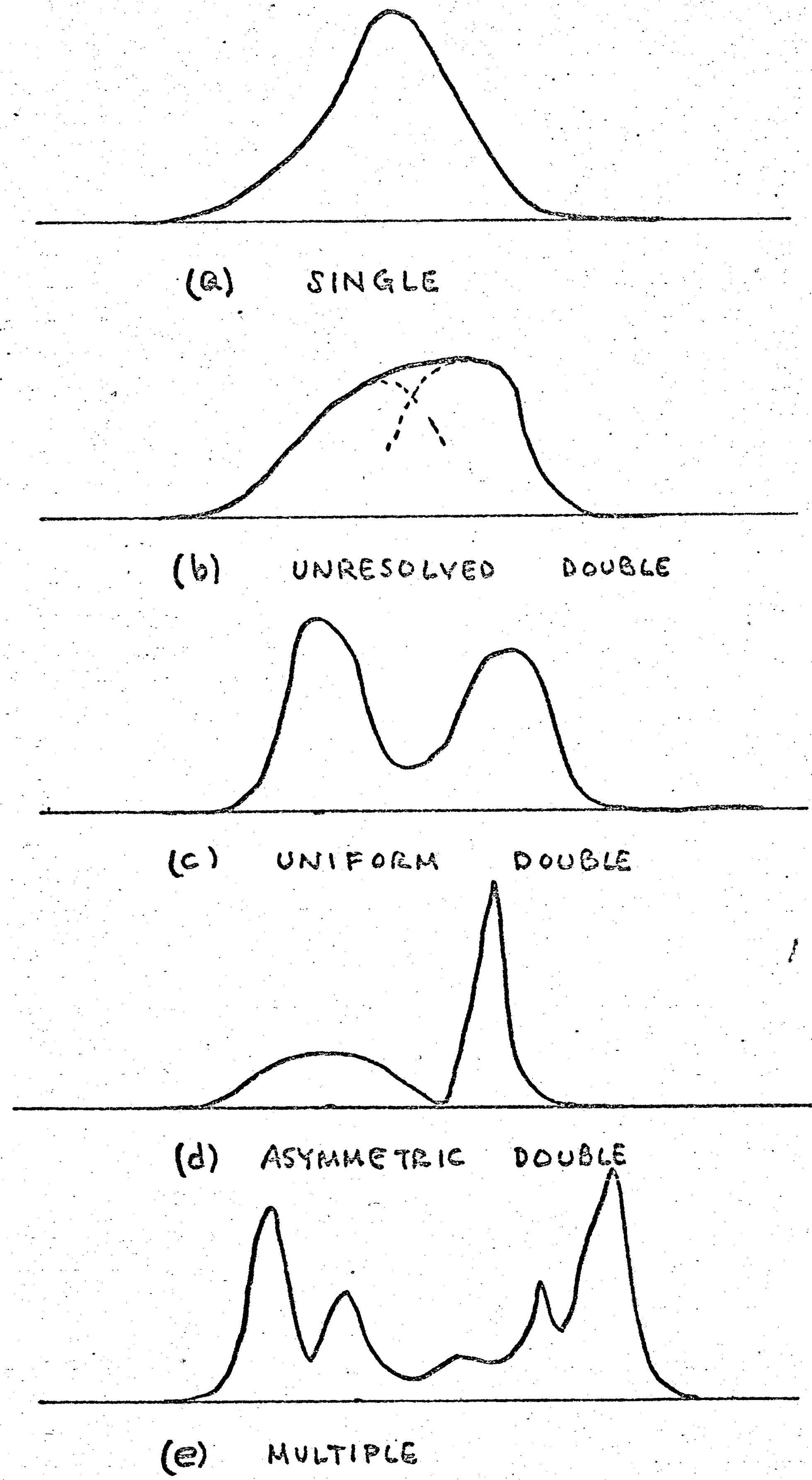

Pulse Profiles. Five varieties of observed pulse profiles with different pulse component structure.

Figure 7

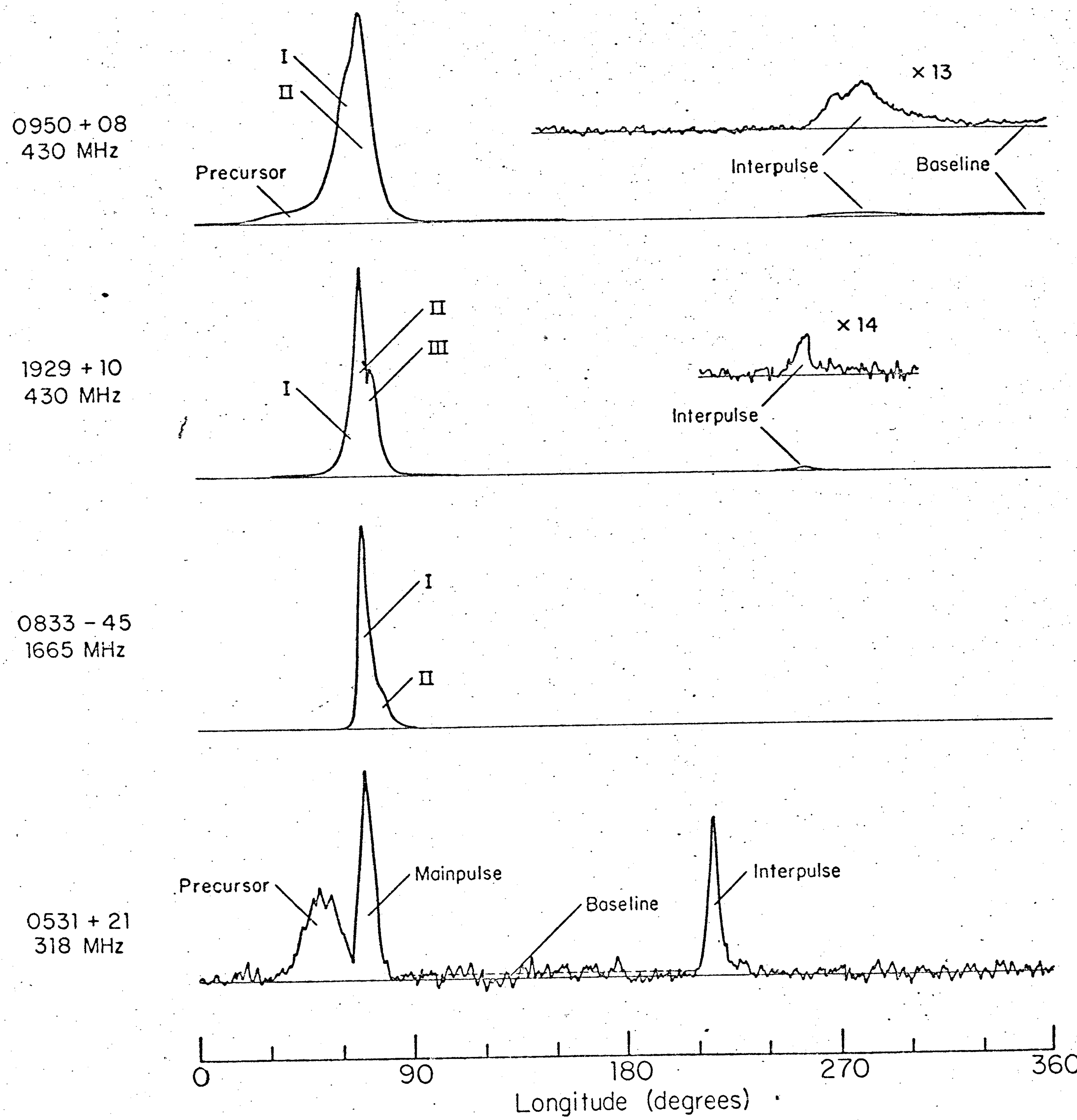

Pulse Profiles. The full period emission profiles of four short period pulsars are shown ($P < 0.25s.$). Three have interpulse components.

Figure 8